

# Direct imaging of crystallographic tilting for valley-controlled Si/SiGe qubits

Koichi Takeuchi<sup>1</sup>, Satoru Miyamoto<sup>1,2,\*</sup>, Kohei M. Itoh<sup>2</sup>, Noritaka Usami<sup>1</sup>

<sup>1</sup> Graduate School of Engineering, Nagoya University  
Furo-cho, Chikusa-ku, Nagoya 464-8603, Japan

<sup>2</sup> School of Fundamental Science and Technology and Spintronics Research Center, Keio University  
3-14-1 Hiyoshi, Kohoku-ku, Yokohama 223-8522, Japan  
Phone: +81-52-789-3243, \*E-mail: miyamoto.satoru@material.nagoya-u.ac.jp

## Abstract

In silicon-based quantum computer, valley splitting can be suppressed due to the presence of atomic-scale steps at spin-qubit integrated interface. For preparation of well-separated and controlled valley branches, we address crystallographic tilting effects on our isotopically engineered Si-28/SiGe quantum-well architectures. Direct imaging based on transmission electron microscope provides us a simple approach to determine local tilting angles at nanoscale resolution. As a result, it is shown that local step fluctuations at the interface are most relevant to dislocation networks in the underlying SiGe buffer layers.

## 1. Introduction

Isotope engineering in silicon semiconductor provides a strong boost to development of Si-based quantum computing [1]. Following successful demonstrations of proof-of-concept experiments utilizing the standard CMOS nano-electronic devices of gate-controlled Si quantum dots and donors [2, 3], the state-of-the-art in isotope engineering was adopted to strained-Si/SiGe quantum-well (QW) architectures, where prolonged coherence enabled to demonstrate gate fidelity exceeding 99.9% [4]. Despite spatial separation of the qubit-integrated layer from gate-oxide interface traps, temporal charge fluctuations in the embedded structures remain as a critical issue for an electrical qubit control on the basis of spatial oscillation.

In addition, Si-based spin qubits are potentially perturbed by the remaining two-fold valley degeneracy, whose energy splitting is needed to be large enough that the lowest valley states are well-separated from the upper branches. For the Si/SiGe system, several theoretical studies showed that the valley splitting is subject to a phase difference of confined electron spreading across an atomic-scale step at the QW interface [5]. This fact defines a structural requirement for the Si/SiGe QW architecture; a lateral step separation should be sufficiently enlarged compared to qubit-integrated scales. In principle, while the epitaxial growth proceeds accompanying both strain relaxation and plastic distortion, a crystallographic orientation is tilted from a normal direction, and consequently atomic-scale step variations are generated at the Si-QW interface. Recent advances in X-ray nano-diffraction indeed lead to spatially-resolved investigations on the structural tilting effects in the Si/SiGe QWs [6]. More recently, transport experiments in quantum-Hall regime indicates that the valley splitting can be effectively suppressed by an

increased step density at the interface [7].

So far, we demonstrated large valley splitting up to several hundred  $\mu\text{eV}$  for our isotopically enriched Si-28/SiGe QWs [8]. However, the origin of the valley-splitting enhancement is not fully understood at present. In this work, we present direct investigation of local crystallographic tilting based on transmission electron microscope (TEM).

## 2. Experimental method

6-inch Si (001) wafers having a nominal miscut  $\alpha_{\text{Si}} < \pm 1^\circ$  were used to prepare two different types of SiGe virtual substrates, which possess a few visible threading dislocations (Sample I) and efficiently confined dislocation networks (Sample II), respectively. As shown in Fig. 1(a), both types of  $\text{Si}_{1-x}\text{Ge}_x$  graded buffer basically consist of continuous layers having linearly increased Ge concentration up to  $x_{\text{Ge}} \sim 30\%$  over a total thickness of  $\sim 3 \mu\text{m}$ , and on top of that the SiGe relaxed buffer layer was deposited at constant  $x_{\text{Ge}}$ . In order to remove surface height variations, surface planarization was carried out by standard chemical mechanical polishing. Subsequently, the same sequence was adopted for regrowth on the polished substrates; the regrowth of  $\text{Si}_{0.7}\text{Ge}_{0.3}$  buffer layer was followed by deposition of the 10-nm-thickness Si-28 QW capped with  $\text{Si}_{0.7}\text{Ge}_{0.3}$  and uppermost Si layers. Since

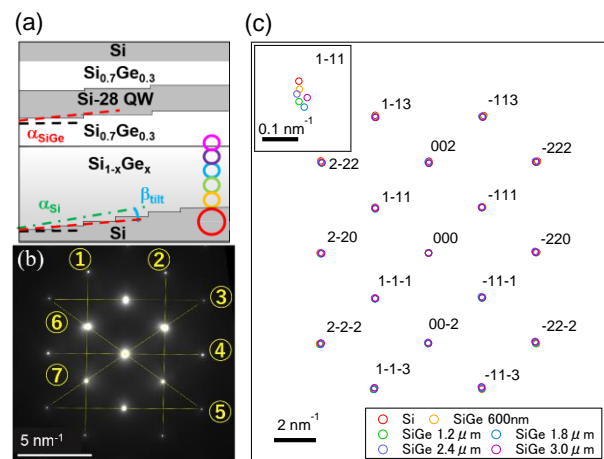


Fig. 1 (a) Schematic illustration of the investigated Si-28/Si<sub>0.3</sub>Ge<sub>0.7</sub> QWs. The circles represent selected areas for local tilting measurements. (b) Typical TEM diffraction pattern obtained from the underlying Si substrate. The seven dashed lines are used for tilting analysis. (c) Diffraction spot positions extracted from the corresponding regions in (a). The magnified displacements of the (1-11) diffraction spots are shown in the inset.

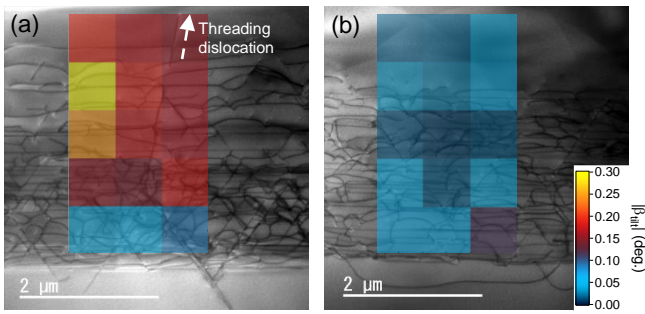


Fig. 2 Tilting amplitude mappings superimposed on cross-sectional TEM images for (a) Sample I and (b) Sample II. The Si-28 QW layers are not shown in the observed areas.

the crystallographic tilting was considered to take place mainly during the SiGe buffer growth, a series of TEM diffraction patterns were recorded from selected areas along the depth direction [see Fig. 1(a)]. Figure 1(b) is a typical diffraction pattern taken from the underlying Si substrate, and then the local tilting of the upper SiGe buffer layers  $\beta_{\text{tilt}}$  was extracted from a rotation angle of each corresponding diffraction spot with respect to the center direct spots. As shown in Fig. 1(b), several lines connecting higher-index diffraction spots were selected to increase the resolution for the calculated angles, where the spot positions were analyzed by a general moment calculation method. For reference, the global tilting averaged over the in-plane directions was also examined for the SiGe relaxed layers using conventional X-ray macro-diffraction. Then the total reflection condition was used for alignment of sample surface.

### 3. Results and discussion

Figure 1(c) displays the spot positions of diffraction patterns taken at different distances from the Si substrate. Slight displacements of the spot positions reflect local variations in lattice distortion as well as in tilting angle. Here, the local tilting amplitude  $|\beta_{\text{tilt}}|$  can be analyzed on the basis of the procedures described above. Figures 2(a) and 2(b) show the cross-sectional TEM images for the two different samples, respectively, where the local  $|\beta_{\text{tilt}}|$  is simultaneously mapped out in various regions. It is clearly seen that Sample I contains more noticeable threading dislocations, while Samples II forms dislocation networks confined in the SiGe graded buffer layer. Obviously, Sample I exhibits an overall  $|\beta_{\text{tilt}}|$  increase in the direction of the surface side, which suggests that the local tilting effects are more pronounced due to strain relaxation during the graded-buffer growth. In addition,  $|\beta_{\text{tilt}}|$  seems to be locally modulated in the proximity of threading dislocations, whereas Sample II having less threading dislocation shows no significant change in  $|\beta_{\text{tilt}}|$ . Thus, it is most likely that the presence of threading dislocation promotes the local crystallographic tilting of the graded buffer layer.

In order to confirm the validity of the above TEM investigations, we carried out the XRD measurements to determine the global  $\beta_{\text{tilt}}$ , as well as the miscut angles for the SiGe relaxed buffer layer and Si substrate, i.e.  $\alpha_{\text{SiGe}}$  and  $\alpha_{\text{Si}}$ .

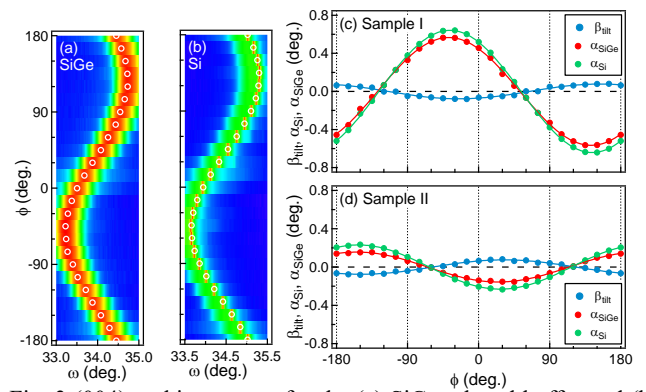


Fig. 3 (004) rocking curves for the (a) SiGe relaxed buffer and (b) Si substrate regions obtained with varying the azimuth angle  $\phi$  (Sample I). The peak positions are marked by the circles in each panel. (c)(d)  $\phi$ -dependent variations in the global parameters,  $\beta_{\text{tilt}}$ ,  $\alpha_{\text{SiGe}}$ , and  $\alpha_{\text{Si}}$ , calculated for the respective samples. The solid lines are given by a sinusoidal fitting.

Figures 3(a) and 3(b) show the (004) rocking curves around the SiGe relaxed buffer and Si substrate peaks measured with rotating an azimuth angle  $\phi$ . The peak positions then yield the global parameters,  $\beta_{\text{tilt}}$ ,  $\alpha_{\text{SiGe}}$ , and  $\alpha_{\text{Si}}$ , for each region [Figs. 3(c) and 3(d)]. The  $\phi$ -dependent curves are well-fitted with a sinusoidal function, whose phase tells us the  $\phi$  direction of surface tilting. Considering that the TEM diffraction is observed in the [110] incident direction, it is found that the local  $\alpha_{\text{SiGe}}$  shows a good agreement with the global  $\alpha_{\text{SiGe}}$ , within a reasonable deviation originating from local tilting fluctuations. For instance,  $|\alpha_{\text{SiGe}}|$  is  $\sim 0.2\text{-}0.4^\circ$  (Sample I) and  $\sim 0.07\text{-}0.14^\circ$  (Sample II), and then the lateral step separations at the interface are predicted to be on the order of  $s \sim 30$  nm and  $\sim 80$  nm, respectively. Assuming that a typical spin-qubit scale is approximately 30 nm for Si quantum dots, it is expected that the valley splitting may be more enhanced for Sample II.

### 4. Conclusions

We presented direct observation of the local tilting effects for the Si/SiGe QW architectures, by means of the TEM diffraction. Tuning the magnitude of valley splitting via atomic-scale step density should provide an additional controllability for scalable Si-based quantum computers.

### Acknowledgements

This work was supported by MEXT Quantum Leap Flagship Program (MEXT Q-LEAP) Grant Number JPMXS0118069228 and Spintronics Research Network of Japan.

### References

- [1] K. M. Itoh *et al.*, MRS Communications **4**, 14 (2014).
- [2] M. Veldhorst *et al.*, Nat. Nanotechnol. **9**, 981 (2014).
- [3] J. T. Muhonen *et al.*, Nat. Nanotechnol. **9**, 986 (2014).
- [4] J. Yoneda *et al.*, Nat. Nanotechnol. **13**, 102 (2018).
- [5] M. Friesen *et al.*, Phys. Rev. B **75**, 115318 (2007).
- [6] S. F. Neyens *et al.*, Appl. Phys. Lett. **112**, 243107 (2018).
- [7] P. G. Evans *et al.*, Adv. Mater. **24**, 5217 (2012).
- [8] S. Miyamoto *et al.*, IEDM - Technical Digest p.p. 6.4.1-6.4.4 (2018).